Supplemental Information

Supplemental Data

Figure S1, Related to Figure 1

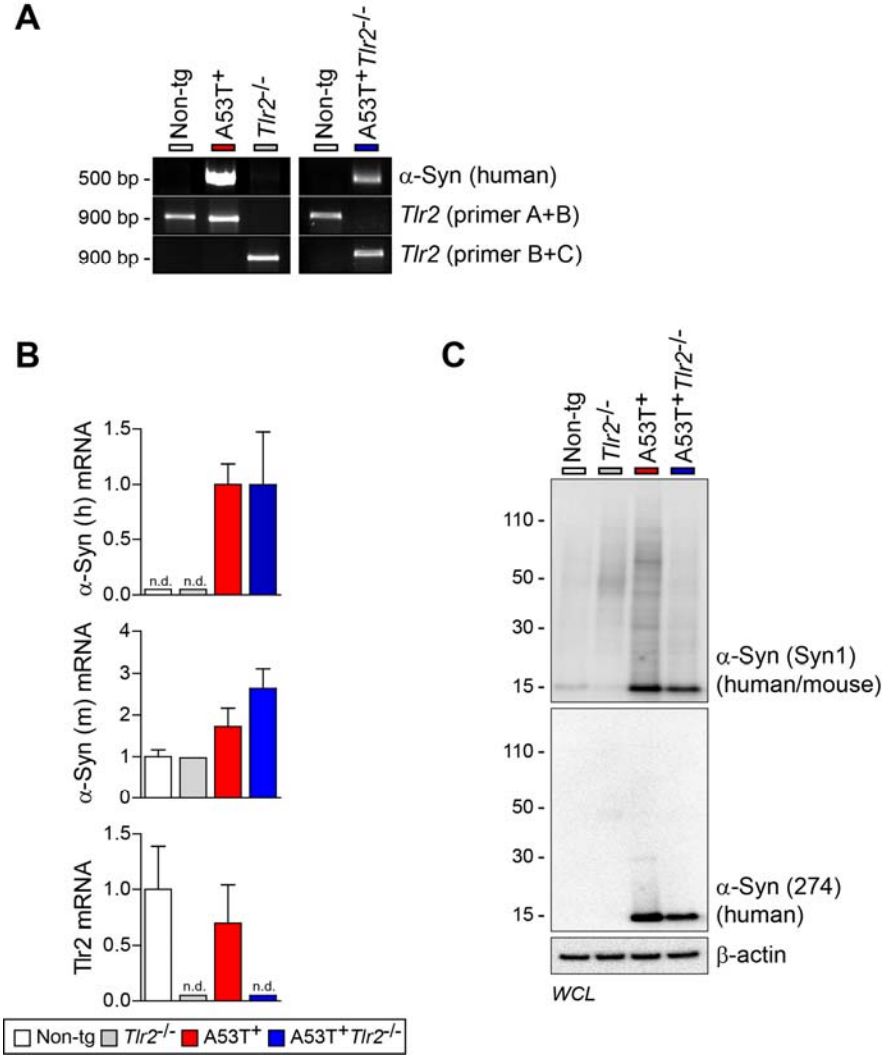

Figure S1. Genotyping and Gene Expression Analysis of A53T^{+}*Tlr2*$^{-/-}$ Double Transgenic Mice

(A) PCR genotyping of mice was performed with specific primers for human α-synuclein and mouse *Tlr2*.

(B) Gene expressions of human α-synuclein, endogenous mouse α-synuclein, and endogenous mous Tlr2 were determined by real-time PCR (non-tg, n = 3; Tlr2-/-, n = 1; A53T+, n = 3; A53T+Tlr2-/-, n = 2; n.d., not detected).

(C) Whole brain lysates from non-tg and tg mice were analyzed by western blot analysis for human α-synuclein, total α-synuclein, and β-actin.

Figure S2, Related to Figure 2

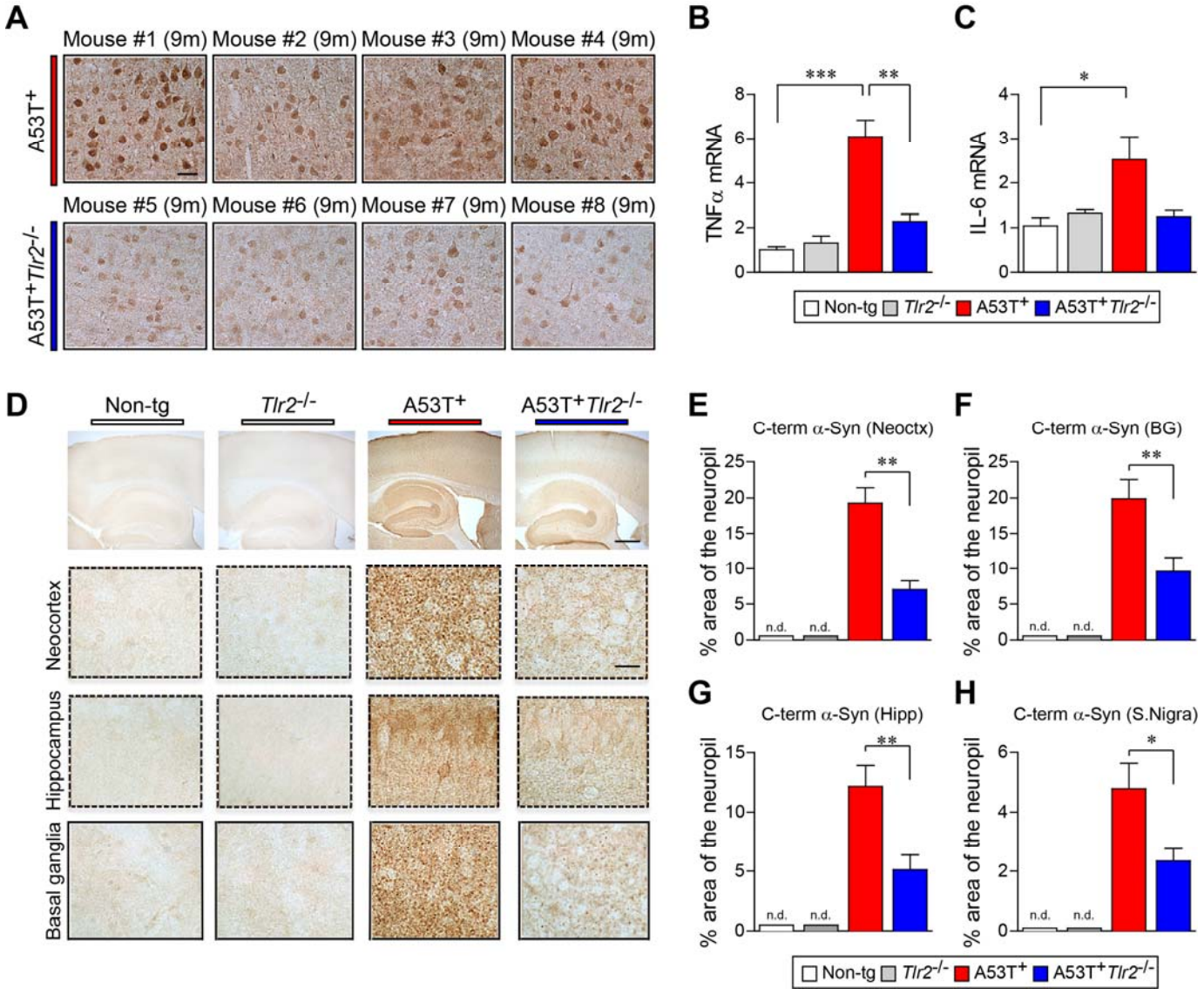

Figure S2. Deposition of α-synuclein and Cytokine Gene Expression in Transgenic Mice Brains

Mice brain sections were inmmunostained against total α-synuclein (Syn-1 antibody) or C-terminal of human α-synuclein (Syn105 antibody).

(A) Representative images of α-synuclein in the neocortex of 9-month-old A53T^{+} (upper panels) and A53T^{+}*Tlr2*$^{-/-}$ (lower panels) mice brains. Scale bar, 25 μm.

(B and C) Expression levels of TNFα (B) and IL-6 (C) in the cortices of non-tg and tg mice were determined by quantitative PCR (n = 4 per group; one-way ANOVA; *p < 0.05, **p < 0.01, ***p < 0.001). Data are represented as mean ± SEM.

(B) Representative images of human α-synuclein (Syn105) in neocortex, basal ganglia, hippocampus, and substantia nigra of non-tg and tg mice brains. Scale bars, 250 μm (low magnification) and 25 μm (high magnification).

(C-F) Optical density analysis of human α-synuclein (Syn105) in neocortex, basal ganglia, hippocampus, and substantia nigra of 6-month age-matched non-tg and tg mice brains (n = 6 per group; one-way ANOVA; *p < 0.05, **p < 0.01). Data are represented as mean ± SEM.

Figure S3, Related to Figure 3

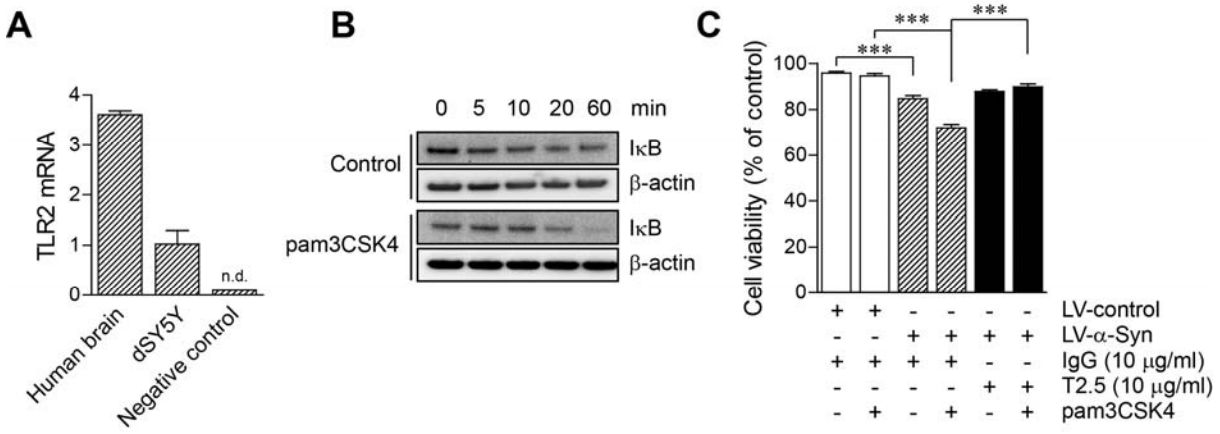

Figure S3. Expression of TLR2 in Neuronal Cells

(A) Expression of human TLR2 in neuronal cells was determined by quantitative realtime PCR. Total mRNAs were extracted from human brains (positive controls), mice brains (negative controls), and dSY5Y cells (n = 4; n.d., not detected). Data are represented as mean ± SEM.

(B) TLR2 ligand response assay in dSY5Y cells. Cells were treated with TLR2 specific agonist (pam3CSK4, 10 μg/ml) for indicated time. Whole cell lysates were analyzed by western blot analysis for IκB.

(C) Cell viability analysis in dSY5Y cells. dSY5Y cells were infected with either LV-control or LV-α-Syn, and treated with IgG (10 μg/ml) or T2.5 (10 μg/ml). After 30 minute incubation, cells were treated with pam3CSK4 (10 μg/ml) for 24 hours. (n = 4 per group; one-way ANOVA; ***$p < 0.001$). Data are represented as mean ± SEM.

Figure S4, Related to Figure 3 and 4

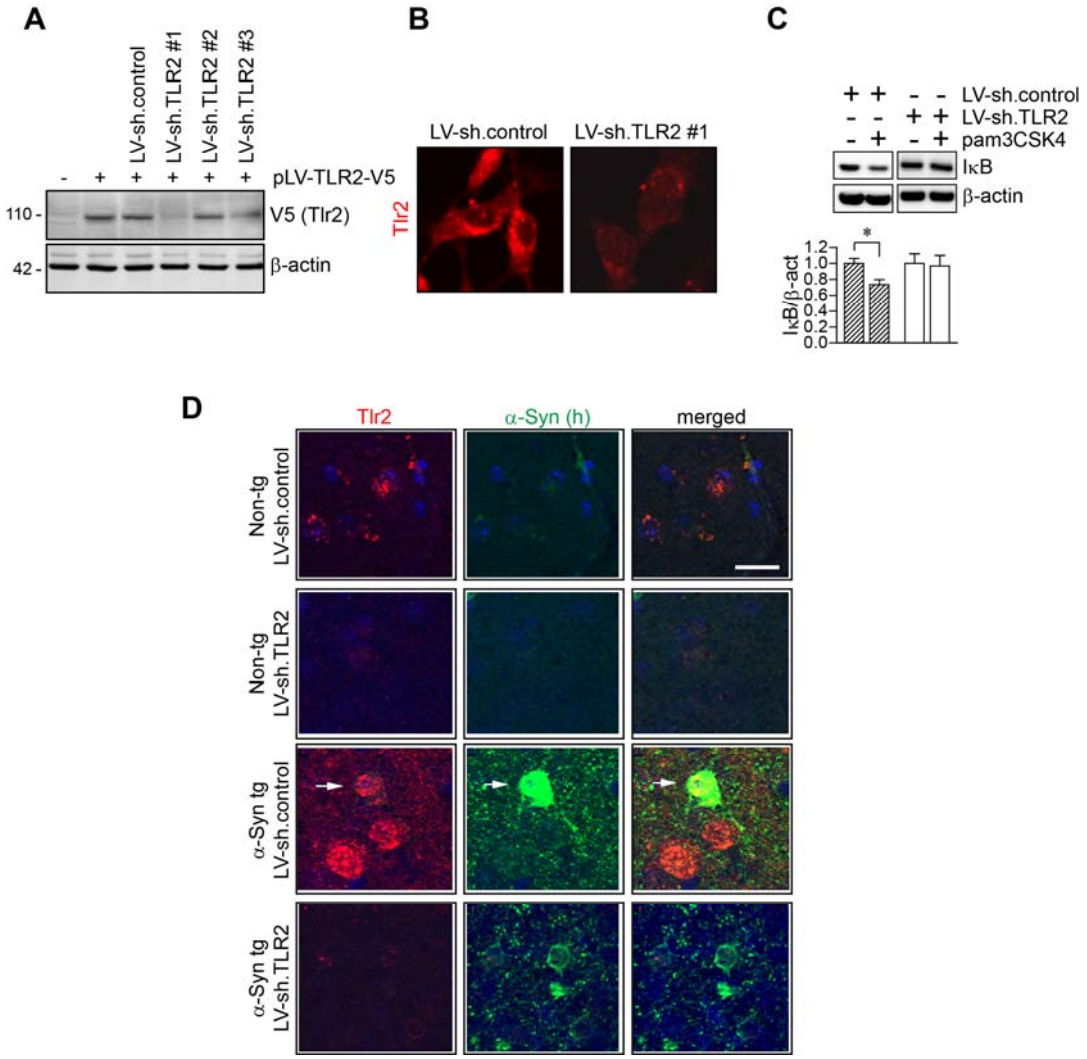

Figure S4. Construction and selection of TLR2 knockdown lentiviral vector

(A) Western blot analysis for TLR2 in 293T cells. Cells were transfected with pLV-TLR2-V5, than infected with LV-sh.control, LV-sh.TLR2 #1, LV-sh.TLR2 #2, and LV-sh.TLR2 #3. Whole cell lysates were analyzed by western blot analysis for Tlr2 (V5 tag).

(B) Representative images for Tlr2 in B103 neuronal cells. Cells were transfected with pLV-TLR2-V5, and infected with LV-sh.control or LV-sh.TLR2 #1 and then immunostained for Tlr2.

(C) Knockdown of TLR2 inhibits pam3CSK4-mediated TLR2 downstream signaling cascade. dSY5Y cells were infected with either LV-sh.control or LV-sh.TLR2, and treated with pam3CSK4 (10 μg/ml) for 60 minutes. Whole cell lysates were analyzed by western blot analysis for IκB (n = 4; unpaired *t*-test; *p < 0.05). Data are represented as mean ± SEM.

(D) Representative images for Tlr2 and α-synuclein of non-tg and α-Syn tg (D line) mice brains (cortex). Lentiviral vectors (LV-sh.control and LV-sh.TLR2) were injected into right hippocampus and right striatum of non-tg and tg mice. After 5-weeks post injection, brain sections were co-immunolabeled with Tlr2 and α-synuclein antibodies (Syn211). Scale bar, 25 μm.

Figure S5, Related to Figure 5

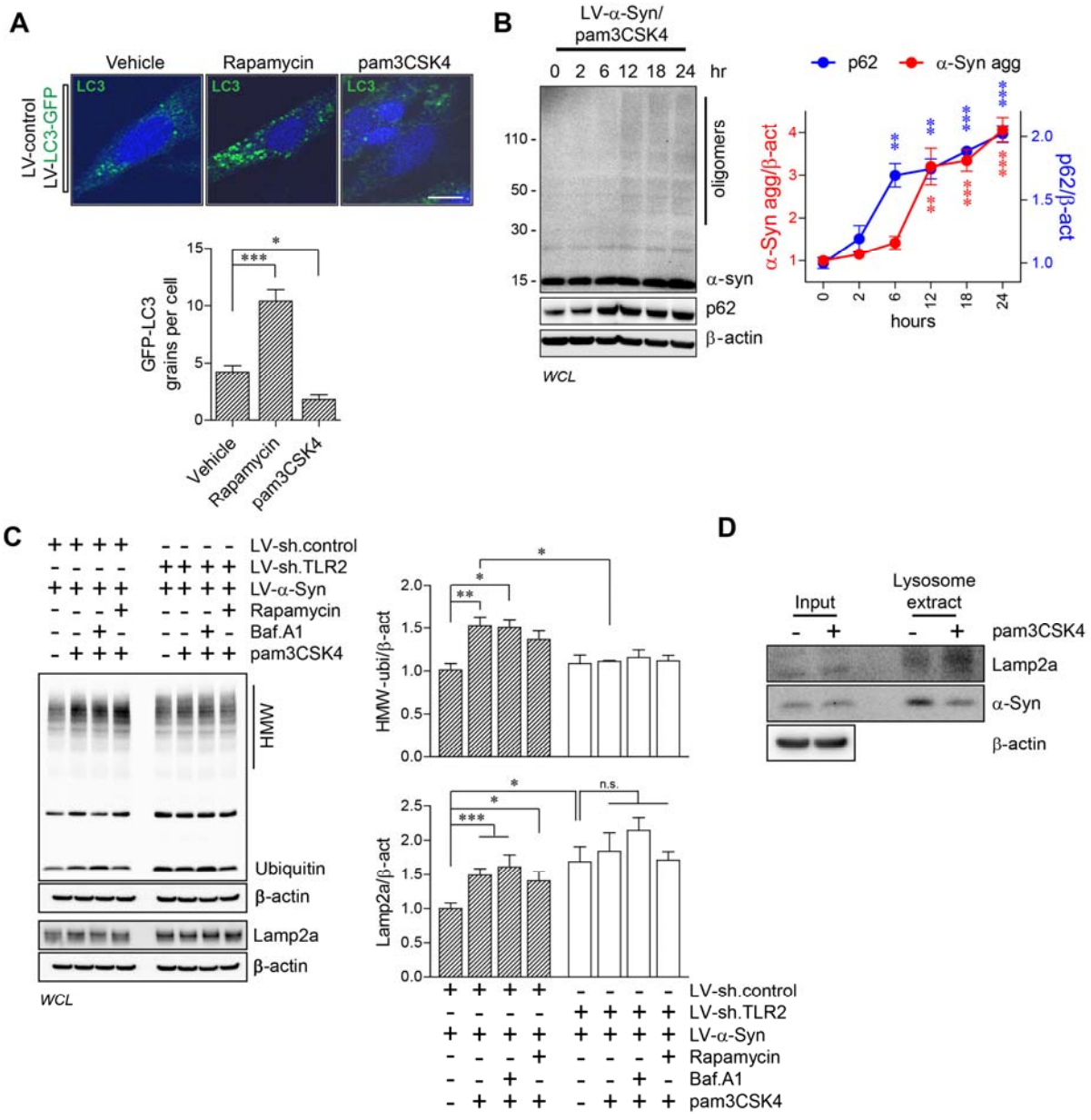

Figure S5. Impairment of Autophagy by TLR2 Activation Occurred Prior to Accumulation of α-synuclein Oligomers and Leading to Lysosomal Alterations in Neuronal Cells

(A) dSY5Y cells were infected with LV-control and LV-LC3-GFP, and treated with rapamycin (100 μM) or pam3CSK4 (10 μg/ml) for 24 hours. Formations of LC3-GFP grains (green) and nuclei (DAPI, blue) were analyzed by confocal microscope. LC3-GFP grains were analyzed in ten randomly chosen

areas from three independent experiments (n = 3; one-way ANOVA; *p < 0.05). Data are represented as mean ± SEM. Scale bar, 20 μm.

(B) dSY5Y cells were infected with LV-α-Syn and treated with pam3CSK4 (10 μg/ml) for indicated hours. Whole cell lysates were analyzed by western blot for α-synuclein and p62/SQSTM1, and the levels of α-synuclein oligomers and p62/SQSTM1 were determined by densitometric quantification (n = 3; one-way ANOVA; **p < 0.01, ***p < 0.001). Data are represented as mean ± SEM.

(C) dSY5Y cells were infected with either combination of LV-α-Syn/LV-sh.control or LV-α-Syn/LV-sh.TLR2, then treated with pam3CSK4 (10 μg/ml) and/or rapamycin (100 μM) for 24 hours. Bafilomycin A1 (Baf.A1, 100 nM) was added for 30 minutes before adding pam3CSK4. Whole cell lysates were analyzed by western blot analysis for ubiquitinated proteins and Lamp2a. The levels of high molecular weight ubiquitinated proteins and Lamp2a were determined by densitometric quantification (n = 3; one-way ANOVA; *p < 0.05, **p < 0.01, ***p < 0.001; n.s., not significant). Data are represented as mean ± SEM.

(D) V1S cells were treated with pam3CSK4 (10 μg/ml) for 24 hours, and the lysosomes were isolated and analyzed by western blot analysis for Lamp2a and α-synuclein.

Figure S6, Related to Figure 5

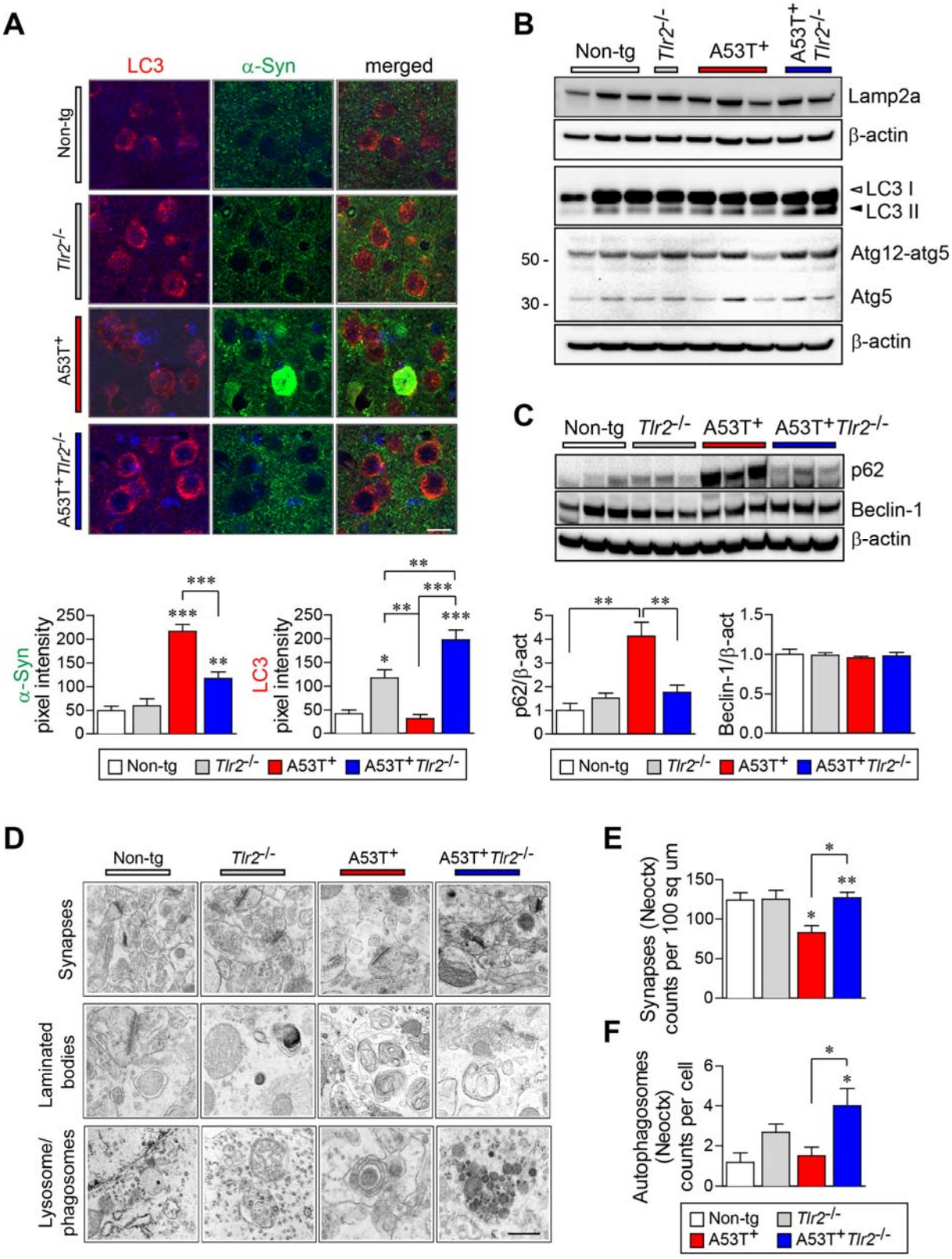

Figure S6. Tlr2-dependent Impairment of Autophagy and Neurodegeneration in α-synuclein Transgenic Mice

(A) Brain sections from frontal cortex of 9-month age-matched non-tg and tg mice were double labeled with α-synuclein and LC3 antibodies. Optical density analysis of immunohistochemical immunoreactivity of α-synuclein and LC3 (n = 6 per group; one-way ANOVA; *p < 0.05, **p < 0.01, ***p < 0.001). Data are represented as mean ± SEM. Scale bar, 25 μm.

(B) Western blot analysis of whole brain homogenates (frontal cortex) for autophagy markers.

(C) The levels of p62/SQSTM1 and beclin-1 in the brain homogenates (the frontal cortices). (n = 3 per group; one-way ANOVA; **p < 0.01). Data are represented as mean ± SEM.

(D-F) Cortex of 9-month age-matched non-tg and tg mice brains were analyzed by electron microscopy analysis for synaptic degeneration and formation of autophagosomes.

(D) Representative images of electron microscopy of non-tg and tg mice brains.

(E and F) The numbers of synapses and autophagosomes were analyzed in 100 sq μm area and per cells respectively (n = 6 per group; one-way ANOVA; *p < 0.05, **p < 0.01). Data are represented as mean ± SEM. Scale bar, 0.5 μm.

Figure S7, Related to Figure 7

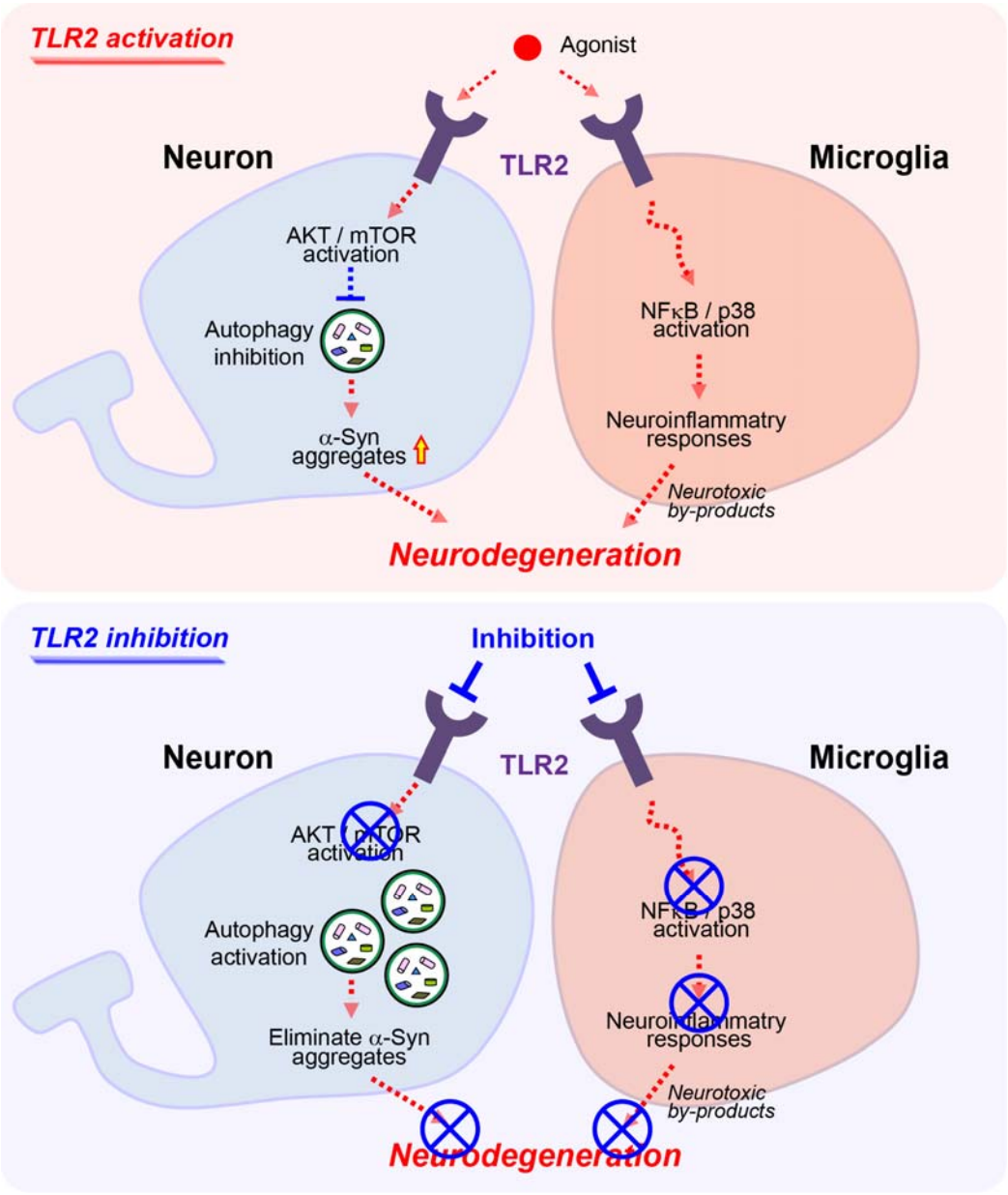

Figure S7. Dual Pathological Roles of TLR2 in Neuron and Microglia, Related to Figure 7

Activation of TLR2 induces accumulation of α-synuclein oligomers resulted in neurodegeneration through TLR2/AKT/mTOR signaling-dependent autophagy failure in neurons. Microglial TLR2 activation also induces neuroinflammation through TLR2/NFκB signaling pathway; which produces neurotoxic by-products, such as inflammatory cytokines, nitric oxides, and reactive oxygen species.

Regulation of TLR2 may be a therapeutic target that can act on both neurons and glia, relieving both synucleinopathy lesions and neuroinflammation.

Table S1. Primers and Reaction Conditions for PCR Analysis, Related to Figure 1, 6, and Experimental Procedures

(F) forward primer, (R) reverse primer.

Genes			Sequence (5' to 3') / TaqMan ID	Species	Application
1	α-synuclein	F	TGGCAGAAGCAGCAGGAAAG	Human	Realtime PCR
		R	AGCCACTGTTGCCACACCAT		
2	α-synuclein	F	CCATGGCGTACAAGTGCTCA	Mouse	Realtime PCR
		R	CAGGTACAGGACGCCGATCA		
3	Tlr2	F	CTGGAGCCCATTGAGAGGAA	Mouse	Realtime PCR
		R	AAGGGCCACTCCAGGTAGGT		
4	β-actin	F	CAGGTCTGAGGCCTCCCTTTT	Mouse	Realtime PCR
		R	GCTGCCTCAACACCTCAACC		
5	IL-6		Mm00446190_m1 (TagMan ID)	Mouse	Realtime PCR
6	TNF-α		Mm00443258_m1 (TagMan ID)	Mouse	Realtime PCR
7	TLR2		Hs01872448_s1 (TagMan ID)	Human	Realtime PCR
8	β-actin		Hs99999903_m1 (TagMan ID)	Human	Realtime PCR
9	α-synuclein (A53T)	F	GGCACCTAGAGGATCTCGACTAGTGG	Human	Genotyping
		R	GGACCTCGACGCTTAGGCTTCAGG		
10	Tlr2	A	GTTTAGTGCCTGTATCCAGTCAGTGC	Mouse	Genotyping
		B	TTGGATAAGTCTGATAGCCTTGCCTCC		
		C	ATCGCCTTCTATCGCCTTCTTGACGAG		

Supplemental Experimental Procedures

Antibodies and Chemicals

The protease inhibitor cocktail and phosphatase inhibitors were purchased from Sigma-Aldrich (St Louis, MO). pam3CSK4 was obtained from InvivoGen (San Diego, CA). GSK690693 was purchased from Selleckchem (Huston, TX). The following antibodies were used: α-synuclein (Syn-1; BD Bioscience, San Diego, CA); polyclonal α-synuclein antibody, GFAP (GA5), and NeuN (Millipore, County Cork, Ireland); TLR2 (clone T2.5) and IgG (eBioscience, San Diego, CA); TLR2 and Lamp2a (Abcam, Cambridge, MA); p62/SQSTM1 and β-actin (Sigma-Aldrich, St Louis, MO); Beclin-1, Atg5, IκB, AKT, phospho-AKT (S473), and phospho-mTOR (S2481) (Cell signaling, Beverly, MA); α-synuclein (274) (Lee et al., 2011); α-synuclein (CT, Syn105) (Games et al., 2014); α-synuclein (syn211) (Life Technologies, Grand Island, NY); Ubiquitin (Dako, Carpinteria, CA); LC3 (MBL international, Woburn, MA); Iba-1 (Wako, Richimond, VA).

Cell Culture and Infection of Lentiviral Vectors

Human SH-SY5Y neuroblastoma cells and V1S-SY5Y cells were maintained and differentiated according to a previously described protocol (Bae et al., 2014; Kim et al., 2013). Maintenance of HEK 293T and B103 neuroblastoma cells have been previously described (Kim et al., 2013; Spencer et al., 2014). Neural precursor cells (NPCs) were differentiated and isolated from induced pluripotent stem cells (GM/Ctl line, Coriell Institute) according to previously described protocol (Boyer et al., 2012; Brafman et al., 2013). Construction and preparation of lentiviral vectors (LV-control, LV-α-Syn, LV-LC3-GFP, and LV-GFP) have been previously described (Spencer et al., 2014). Murine Atg7 (Open

Biosystems, Lafayette, CO) and LC3-GFP-mCherry (Addgene, Cambridge, MA) were cloned into the 3rd generation lentivector under the control of the human CMV promoter to generate LV-Atg7 and LV-GFP-mCherry respectively. LV-siAtg7 was generated by cloning the sequence GCA TCA TCT TTG AAG TGAA corresponding to nucleotides 833-855 of murine Atg7 into the vector pSIH1-copGFP (Systems Bioscience) under the control of the human H1 promoter. LV-siTLR2 was generated from analysis of the murine TLR2 cDNA using the sFold algorithm to generate the following siRNAs: #1 CCA ATC TCA CAA ATT TACA, #2 ACA ACA ATC TTG ACT CATT, #3 CTG CAA ACT GCG CAA GATA. The three shRNA sequences were cloned into the pSIH1-copGFP vector and tested by co-transfection with the TLR2-V5 expression plasmid for knockdown of murine TLR2. To deliver lentiviral vectors, dSY5Y and NPCs were infected with viral vectors at multiplicity of infection of 100 (LV-control, LV-GFP, and LV-α-Syn), 50 (LV-sh.control, LV-sh.TLR2, LV-sh.ATG7, and LV-ATG7), and 20 (LV-LC3-GFP and LV-LC3-GFP-mCherry).

Quantitative Polymerase Chain Reaction

Total RNAs were extracted from mice brains (9-month-old) using RNeasy Lipid mini kit (Qiagen, Germantown, MD) and reverse transcribed using SuperScript VILO cDNA synthesis kit (Life Technologies), respectively. Quantitative real-time PCR was performed using TaqMan® Fast Advanced Master Mix (Life Technologies) according to manufacturer's instruction with gene specific primers (Table S1). Amplification of DNA products was measured by the StepOnePlus real-time PCR system (Applied Biosystems, Carlsbad, CA). Relative mRNA levels were calculated according to the 2-exp ($\Delta\Delta$Ct) method. All ΔC_T values were normalized to β-actin.

Preparation of Cell and Tissue Extracts, and Western Blot Analysis

The procedures for cell/tissue extract preparation and western blot analysis have been described elsewhere (Lee and Lee, 2002; Spencer et al., 2014). Briefly, cells and brain homogenates (9 month) were prepared in the lysis buffer (1% Triton X-100/PBS and protease-phosphatase inhibitor mixture) to separate Tx-soluble and Tx-insoluble fractions. To obtain whole cell lysates, cell and brains extracts were lysed with Laemmle sample buffer (Life Technologies). Chemiluminescence detection and analysis were performed using a Versadoc XL imaging apparatus and Quantity One (Bio-rad, Hercules, CA).

Electron Microscopy Analysis

Vibratome sections of mice brains were post fixed in 1% glutaraldehyde, treated with osmium tetraoxide, embedded in epon araldite and sectioned with an ultramicrotome (Leica, Germany). Grids were analyzed with a Zeiss ON 10 electron microscope as previously described (Spencer et al., 2009).

Cytotoxicity Analysis

Number of dead cells and viability were determined by Countess automated cell counter (Invitrogen, Carlsbad, CA) according to manufacturer’s instruction.

Beam Break Test

Motor behavior assessment was determined by the beam break test, a general method for locomotor activity (Tatem et al., 2014). Beam breaks were measured using a high density cage rack system (Kinder Scientific, Poway, CA). This system continuously monitored the location of mice in X, Y, and Z coordinate space within the chamber using infrared photo beams with 7 X and 15 Y resolution. To measure the beam breaks, each mouse was placed into the test chamber and data collection began immediately. Total numbers of beam breaks were automatically calculated and recorded in a 10-minute period. Daily training sessions were conducted for 4 trials each day for a period of 4 days after the first day beam break measurement.

Lysosome Extraction

V1S stable cell line expressing N-term Venus tagged α-synuclein was used for lysosome isolation analysis (Bae et al., 2014). Cells were seeded onto 100 mm cell culture dishes and treated with pam3CSK4 for 24 hours. Lysosomes were extracted from 5 dishes of each group using Lysosome Isolation Kit (Sigma-Aldrich) according to the manufacturer's instructions.

Supplemental References

Bae, E.J., Yang, N.Y., Song, M., Lee, C.S., Lee, J.S., Jung, B.C., Lee, H.J., Kim, S., Masliah, E., Sardi, S.P.*, et al.* (2014). Glucocerebrosidase depletion enhances cell-to-cell transmission of alpha-synuclein. Nature communications *5*, 4755.

Boyer, L.F., Campbell, B., Larkin, S., Mu, Y., and Gage, F.H. (2012). Dopaminergic differentiation of human pluripotent cells. Current protocols in stem cell biology *Chapter 1*, Unit1H 6.

Brafman, D.A., Moya, N., Allen-Soltero, S., Fellner, T., Robinson, M., McMillen, Z.L., Gaasterland, T., and Willert, K. (2013). Analysis of SOX2-expressing cell populations derived from human pluripotent stem cells. Stem cell reports *1*, 464-478.

Games, D., Valera, E., Spencer, B., Rockenstein, E., Mante, M., Adame, A., Patrick, C., Ubhi, K., Nuber, S., Sacayon, P.*, et al.* (2014). Reducing C-terminal-truncated alpha-synuclein by immunotherapy attenuates neurodegeneration and propagation in Parkinson's disease-like models. The Journal of neuroscience : the official journal of the Society for Neuroscience *34*, 9441-9454.

Kim, C., Ho, D.H., Suk, J.E., You, S., Michael, S., Kang, J., Joong Lee, S., Masliah, E., Hwang, D., Lee, H.J.*, et al.* (2013). Neuron-released oligomeric alpha-synuclein is an endogenous agonist of TLR2 for paracrine activation of microglia. Nature communications *4*, 1562.

Lee, H.J., and Lee, S.J. (2002). Characterization of cytoplasmic alpha-synuclein aggregates. Fibril formation is tightly linked to the inclusion-forming process in cells. The Journal of biological chemistry *277*, 48976-48983.

Lee, H.J., Suk, J.E., Lee, K.W., Park, S.H., Blumbergs, P.C., Gai, W.P., and Lee, S.J. (2011). Transmission of Synucleinopathies in the Enteric Nervous System of A53T Alpha-Synuclein Transgenic Mice. Experimental neurobiology *20*, 181-188.

Spencer, B., Emadi, S., Desplats, P., Eleuteri, S., Michael, S., Kosberg, K., Shen, J., Rockenstein, E., Patrick, C., Adame, A.*, et al.* (2014). ESCRT-mediated Uptake and Degradation of Brain-targeted alpha-synuclein Single Chain Antibody Attenuates Neuronal Degeneration In Vivo. Molecular therapy : the journal of the American Society of Gene Therapy *22*, 1753-1767.

Spencer, B., Potkar, R., Trejo, M., Rockenstein, E., Patrick, C., Gindi, R., Adame, A., Wyss-Coray, T., and Masliah, E. (2009). Beclin 1 gene transfer activates autophagy and ameliorates the neurodegenerative pathology in alpha-synuclein models of Parkinson's and Lewy body diseases. The Journal of neuroscience : the official journal of the Society for Neuroscience *29*, 13578-13588.

Tatem, K.S., Quinn, J.L., Phadke, A., Yu, Q., Gordish-Dressman, H., and Nagaraju, K. (2014). Behavioral and locomotor measurements using an open field activity monitoring system for skeletal muscle diseases. Journal of visualized experiments : JoVE, 51785.